Sensors & Transducers, Vol. 267, Issue 4, December 2024, pp. 49-56

www.sensorsportal.com

Sensors & Transducers

Published by IFSA Publishing, S. L., 2024
http://www.sensorsportal.com

An Ultimate Hydrodynamic Model for Semiconductor Devices with Arbitrary Band Structure and Surface Effects

Muhammad El-Saba and Mahmoud-Sifeddin Taha
Ain-Shams University, Engineering College, 1 Research Av., 11517 Abbasia, Cairo, Egypt
E-mail: mhs1308@hotmail.com

Received: 10 June 2024 / Revised: 13 December 2024 / Accepted: 23 December 2024
Published: 30 December 2024

Abstract: In this article we present an advanced hydrodynamic model for studying the charge carrier transport in a wide range of semiconductor devices and sensors. The proposed includes the true energy band structure of any semiconductor material and its surface effects. The model has been compared with other transport models, and its primary results are accurate and closer to the more complex approaches, such as Monte Carlo device simulation. One of the most salient features of our model is its great attention of the convection transport and velocity gradients of charge carriers. Therefore, it handles the electron gas shear rate and viscosity near the rough surfaces of semiconductor devices. This is shown to limit the charge carrier mobility near the surface of semiconductor devices in general and the MOSFET nano-devices in particular. According to our knowledge, the electron/hole gas viscosity effects have not been treated yet in the literature of hydrodynamic modelling and simulation of semiconductor devices and sensors.

Keywords: Semiconductor devices, Hydrodynamic model, Electron gas viscosity, Energy band structure. Electron gas viscosity, Surface mobility.

1. Introduction

The hydrodynamic model (HDM) of charge carrier transport in semiconductors has gained a great attention as a compromising approach between classic and full quantum transport models [1]. In spite of its wide spread in the semiconductor industry, as a simulation tool, the HDM has been a target of a lot of criticism [2-10]. To name a few, the exaggerated electron temperature and velocity overshot in nano devices, were reported [5-6]. According to many authors the weak points of the early HDM are mainly attributed to neglecting the band structure effects [7], neglecting the convective part of the average carrier energy [8], and the crude approximations which are used to close the system of hydrodynamic equations (HDE's) [8-10].

In this article, we introduce an advanced HDM, which incorporates the semiconductor band structure effects, the convection transport of charge carriers and the semi-conductor surface effects. The article is organized as follows. In sections 2, 3, and 4 we introduce the proposed HDM and its development and closure procedure. In addition, we present, in section 5 some advanced models of the carrier-energy-dependent physical parameters to be used with the proposed HDM. In section 6, we present some results of simulation and discuss their significance. We also compare our results with Monte Carlo (MC) device simulations. Finally, we present our conclusions in section 7 and a list of references.

2. Development Methodology

We start the development procedure of the proposed HDM from the general moment equation of the Boltzmann transport equation (BTE) for the gas of

charge carriers (electrons or holes) in a semiconductor device [11]. The moment equation is simply obtained by multi-plying the BTE by a physically-meaningful quantity $\psi_j(\boldsymbol{k})$, and integrating both sides over the whole wavevector space ($\boldsymbol{k}$-space) of charge carriers.

$$\frac{\partial}{\partial t}\int_k \psi_j f_v d^3k + \int \psi_j (u_v.\nabla f_v)_j d^3k + \\ + \int \psi_j \left(\frac{F}{\square}.\nabla_k f_v\right) d^3k \;=\; \int \psi_j \left[\frac{\partial f_v}{\partial t}\right]_{col} d^3k, \tag{1a}$$

where $f_v = f_v(\boldsymbol{x},\boldsymbol{k},t)$ is the carrier distribution function in the phase space, which combines the physical space: $\boldsymbol{x} = [x,y,z]^T$, and the carrier wavevector space: $\boldsymbol{k} = [kx,ky,kz]^T$. The subscript '$_v$' stands for '$_n$' for electrons and stands for '$_p$' for holes. Also, $\boldsymbol{u_v}$ is the carrier group velocity ($u_v = h^{-1}dE_v/dk$), where $E_v(k)$ is the carrier (conduction electron or valence holes) energy (band structure. Finally, $\boldsymbol{F}$ is the externally-applied force, and, $\psi_j = \psi_j(\boldsymbol{k})$ is a multiplier weight function. The resulting set of conservation equations has the following general form:

$$\frac{\partial}{\partial t} n\langle\psi_j\rangle + \nabla.\, n\langle u_v \otimes \psi_j\rangle + n\left\langle\frac{F}{\square}.\nabla_k \otimes \right. \\ \left. \otimes\, \psi_j\right\rangle \;=\; \left[\frac{\partial}{\partial t} n\langle\psi_j\rangle\right]_{col} \tag{1b}$$

Here, n is the average carrier density and the angular brackets <..> denote the statistical average over the carrier distribution function in the k-space

$$<\psi(\boldsymbol{k})> = \int z\; \psi(\boldsymbol{k})\, f_v(\boldsymbol{x},\boldsymbol{k},t)\; d^3\boldsymbol{k} \,/\, n, \tag{1c}$$

where $z = 2/(2\pi)^3$ is the density of states in the k-space, and $n = \int z\, f_v(\boldsymbol{x},\boldsymbol{k},t)\; d^3\boldsymbol{k}$. Note that we put $\nabla_k.F = 0$ in the derivation of (1b) from (1a), which is true if the external force $\boldsymbol{F}$ is independent of k or when $\boldsymbol{F}$ *is* normal to $\boldsymbol{k}$. Fortunately, this is the case for both electric field force ($\boldsymbol{F} = \pm e\,\boldsymbol{\zeta}$, with $\pm e$ being the charge for electrons, or holes and $\boldsymbol{\zeta}$ is the applied electric field), and the Lorentz force ($\boldsymbol{F} = \pm e\; \boldsymbol{v}_n x \boldsymbol{B}$, with $\boldsymbol{B}$ being the magnetic field density). This makes the HDM suitable for studying both conventional semiconductor devices and sensors, which employ (or measure) external magnetic fields. However, in most semi-conductor devices, $\boldsymbol{F}$ is usually due to the applied bias voltages, and therefore, $F = \pm e\boldsymbol{\zeta}$. The electric field, $\boldsymbol{\zeta} = -\nabla\square$, and the electrostatic potential, $\square$, can be found by solving the Poisson equation, using the device boundary conditions of applied bias voltages.

$$\nabla.\,(-\varepsilon\,\nabla\phi + \boldsymbol{P}) = e\,(p - n + Dop + N_t), \tag{1d}$$

where, ε is the dielectric constant, p is the concentration of holes, $\boldsymbol{P}$ is the material polarization vector, N_t is the density of traps and $Dop = |N_d^+ - N_a^-|$ is the net concentration of ionized impurities in the semiconductor.

Our proposed HDM consists of the first three moments of the BTE, with $\psi_j = 1$, the electron group velocity u_n and the electron energy E_n. For simplicity, we only write the first three moments of the BTE for electrons, which represent the conservation equations of the electron average density (n), average momentum (or velocity $\boldsymbol{v}_n$) and average energy (ω_n):

$$\partial n/\partial t \;-\; \nabla.\boldsymbol{J}_n/e) = [\partial n/\partial t]_{col}.., \tag{2a}$$

$$\partial(n\boldsymbol{v}_n)/\partial t + e\; n\; m_n^{-1}\boldsymbol{\zeta} + \nabla.\boldsymbol{\mathcal{P}}_{ne} + \\ + \nabla.(n\;\boldsymbol{v}_n \otimes \boldsymbol{v}_n) = [\partial(n\boldsymbol{v}_n)/\partial t]_{col}, \tag{2b}$$

$$\partial(n\,\omega_n)/\,\partial t + \nabla.S_n = \zeta.\;\boldsymbol{J}_n + (\partial n\omega_n/\partial t\,)_{col} \tag{2c}$$

Here, n is the average density of conduction electrons, $\boldsymbol{v}_n = <\boldsymbol{u}_n>$ is their average velocity, $\square_n = <E_n>$ is their average energy, and $\boldsymbol{\mathcal{P}}_{ne}$ is the electro-kinetic pressure tensor of the electron gas. By definition, $\boldsymbol{\mathcal{P}}_{ne}$ is a second-order central moment, such that:

$$\boldsymbol{\mathcal{P}}_{ne} = n\,<(\boldsymbol{u}_n - \boldsymbol{v}_n)\otimes(\boldsymbol{u}_n - \boldsymbol{v}_n)>, \tag{3a}$$

where the sign $\otimes$ denotes the tensorial product of two vectors. It worth notice that in we expanded the generalized moment term $n <\boldsymbol{u}_n \otimes \boldsymbol{u}_n>$, as follows:

$$n <\boldsymbol{u}_n \otimes \boldsymbol{u}_n > = \boldsymbol{\mathcal{P}}_{ne} + n\,(\boldsymbol{v}_n \otimes \boldsymbol{v}_n) \tag{3b}$$

Also, $\boldsymbol{J}_n = -e\; n\; \boldsymbol{v}_n$ is the electron current density and $\boldsymbol{S}_n = <E_n\boldsymbol{u}_n>$ is the electron energy flux. The average collision terms, denoted by $[..]_{col.}$, at the right-hand side of the three moment equations (2a, b, c). Finally, m_n is the average mass tensor of conduction electrons, whose inverse components are defined as follows:

$$m_n^{-1}{}_{(i,j)} = <1/\hbar^2\,\partial^2 E_n/\partial k_i \partial k_j> \tag{3c}$$

Note that m_n appears naturally in the mathematical derivation of (2b) from the BTE moment equation (1b), and doesn't mean that we adopt the effective mass approximation (EMA) in the above set of hydrodynamic equations (HDE's). (2a, b, c). Actually, m_n is taken as a physical parameter in our HDM, and is considered as a function of the average electron energy ($m_n = m_n(\omega_n)$). At low electron energy, near the conduction band bottom edge, we use the term m_{no} whose value is determined experimentally. For instance, $m_{no} = 0.275m_o$ in Si, according to the optical measurements of Sabbah and Riffe [12].

The electron current density ($\boldsymbol{J}_n$) and energy flux ($\boldsymbol{S}_n$) can be expanded into constitutive relations, from their definitions ($\boldsymbol{J}_n = -e\; n\; \boldsymbol{v}_n$ and $\boldsymbol{S}_n = <E_n\boldsymbol{u}_n>$). We show the expansion procedure in section III, when we close the system of HDE's. The average collision terms in the three moment equations (2a, b, c) are also approximated in the next section.

3. HDM System Closure Procedure

The set of HDE's contains some unknown terms (e.g., the electro-kinetic pressure and collision terms),

whose calculations need the knowledge of the electron distribution function in the phase space, $f_n(\boldsymbol{x},\boldsymbol{k},t)$. However, $f_n(\boldsymbol{x},\boldsymbol{k},t)$ is masked in the HDM development procedure. Therefore, we need some approximate closure conditions to close the system of HDE's.

The HDM system closure assumptions are mainly about approximating and modeling the following items:

- Carrier collision terms;
- Relating the electro-kinetic pressure ($\boldsymbol{P}_{ne}$) to the carrier gas pressure ($\boldsymbol{P}_n$) and the carrier temperature (T_n);
- Expanding the expressions of the carrier current density ($\boldsymbol{J}_n$) and energy flux ($\boldsymbol{S}_n$);
- Relating the average carrier energy (ω_n), to the carrier gas temperature (T_n);
- Modeling the heat flux term ($\boldsymbol{Q}_n$);
- Modeling any higher moment terms (e.g., kurtosis flux and so on), if moments are greater than three.

3.1. Collision Terms

The collision term $[\partial n/\partial t]_{col.}$, which appears explicitly in the carrier density conservation equation (2a), can be expressed as follows:

$$[\partial n/\partial t]_{col.} = -(n-n_o)/\tau_n = -U_n \tag{4a}$$

where τ_n is the lifetime of charge carriers and the net recombination rate ($U_n = R_n - G_n$) combines all the recombination rate (R_n) and generation rate (G_n) mechanisms in the semiconductor.

Because the lifetime of charge carriers is usually much greater than the energy and momentum relaxation times, ($\tau_{mn} << \tau_{wn} << \tau_n$), the collision terms in (2b,c) are usually approximated as follows:

$$[\partial n/\partial t]_{col.} = -(n-n_o)/\tau_n = -U_n, \tag{4b}$$

$$[\partial n\boldsymbol{v}_n/\partial t]_{col.} \approx -n\boldsymbol{v}_n/\tau_{mn} \tag{4c}$$

The energy dependence of the energy relaxation time, $\tau_{wn} = \tau_{wn}(\omega_n)$, which implicitly includes the energy band structure effects, can be obtained by MC simulation in the bulk of a semiconductor [13] or by measurement [14]. On the other hand, the momentum relaxation time (τ_{mn}) is not directly employed in our proposed HDM, but rather replaced with the drift mobility ($\mu_n = e\tau_{mn}/m_n$), whose model is introduced in section V-1.

3.2. Definition of the Carrier Gas Pressure and Temperature

We presume the following relation between the electron gas pressure $\boldsymbol{P}_n$ and its electro-kinetic pressure $\boldsymbol{P}_{ne}$:

$$\boldsymbol{P}_n = m_n\boldsymbol{P}_{ne} \tag{5a}$$

In fact, the ideal gas theory defines the gas pressure, $\boldsymbol{P}_n$, with a *macroscopic (k-independent)* mass density $\rho_n = n\,m_n$, as follows:

$$\boldsymbol{P}_n = \rho_n <(\boldsymbol{u}_n - \boldsymbol{v}_n)\otimes(\boldsymbol{u}_n - \boldsymbol{v}_n)> \tag{5b}$$

Nevertheless, for the matter of compatibility with previous HDM's, where the electron gas pressure is given by: $\boldsymbol{P}_n = n <m_n^*(\boldsymbol{u}_n - \boldsymbol{v}_n)\otimes(\boldsymbol{u}_n - \boldsymbol{v}_n)>$, we introduce here a temperature correction parameter ($\boldsymbol{g}_n$):

$$\boldsymbol{g}_n = m_n\boldsymbol{P}_{ne}\boldsymbol{P}_n^{-1} \tag{6a}$$

Therefore, we rather use the system closure condition:

$$\boldsymbol{P}_{ne} = \boldsymbol{g}_n\, m_n^{-1}\boldsymbol{P}_n \tag{6b}$$

We also adopt the ideal gas law, $\boldsymbol{P}_n = n\,k_B\boldsymbol{T}$, such that:

$$\boldsymbol{P}_{ne} = \boldsymbol{g}_n\, m_n^{-1}\, n\, k_B\boldsymbol{T}_n \tag{6c}$$

The correction parameter can be simplified as the trace of the tensor $\boldsymbol{g}_n = m_n\boldsymbol{P}_{ne}\boldsymbol{P}_n^{-1.}$ where we take the sum of diagonal elements:

$$g_{n(i,i)} = m_{nii} <u_{ni} - v_{ni})^2> / <m_{nii}^*(u_{ni} - v_{ni})^2> \tag{6d}$$

It can be, therefore, calculated by Monte Carlo simulation [15] or modelled as a function of the average electron energy, like m_n and $\tau_{\square n}$. Fig. 1 shows the magnitude of the correction factor, according to Monte Carlo device simulation in the bulk of Si at 300K [15].

(4b)

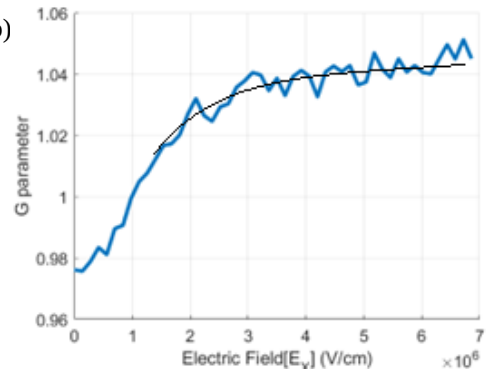

Fig. 1. Variation of the correction factor g_n and its trace versus electric field, as obtained by MC simulation, in the bulk of low-doped Si at 300K [15].

3.3. Current Density Constitutive Relation

The constitutive relations of the electron current density ($\boldsymbol{J}_n$), can be derived from its definition

($\boldsymbol{J}_n$ = -e n $\boldsymbol{v}_n$), using the momentum conservation equation(2b), in steady state

$$\nabla.(\boldsymbol{P}_{ne}) + \nabla.(n\, v_n \otimes v_n) - e\, n\, m_n^{-1}.\boldsymbol{\zeta} + + \left[\frac{\partial n\, v_n}{\partial t}\right]_{col} \quad (7a)$$

Using the momentum relaxation time approximation (4c) and substituting μ_n = eτ_{mn} /m_n and $\boldsymbol{J}_n$ = -e n $\boldsymbol{v}_n$, we get:

$$\boldsymbol{J}_n = e\, n\, \mu_n \boldsymbol{\zeta} + \mu_n\, m_n\ \nabla.\boldsymbol{P}_{ne} + + n\, \mu_n\, m_n\, (v_n.\nabla)\, v_n \quad (7b)$$

Substituting the electro-kinetic pressure ($\boldsymbol{P}_{ne}$) from its closure condition (6d), yields

$$\boldsymbol{J}_n = en\, \mu_n.\boldsymbol{\zeta} + \mu_n.m_n\, \nabla.(g_n\, m_n^{-1}\, n\, k_B T_n) + + n\, \mu_n.m_n(\boldsymbol{v}_n.\nabla)\boldsymbol{v}_n \quad (7c)$$

The above constituent relations are similar to the current density equations of the drift-diffusion model (DDM), except for the velocity gradient (or acceleration) and thermal diffusion terms. Note that the velocity gradient term is vector of three components and nine (3x3) terms, which results from the expansion of ($\nabla.(n\, v_n \otimes v_n)$).

3.4. Electron Energy Flux and Heat Flux

For expanding $\boldsymbol{S}_n$ = <$E_n\boldsymbol{u}_n$>), and ω_n = <E_n>, in terms of the electron temperature (T_n), we make use of the classical definition of electron energy E_n = ½ m_n^* v_n^2 and, therefore, apply the ideal gas laws.

$$\boldsymbol{S}_n = \boldsymbol{Q}_n + \boldsymbol{v}_n(n\, \omega_n + \boldsymbol{P}_n) = \boldsymbol{Q}_n + n\, \boldsymbol{v}_n\, (\omega_n + + k_B T_n), \quad (8a)$$

with

$$\boldsymbol{Q}_n = \int ½\, m_n^* |\boldsymbol{u}_n - \boldsymbol{v}_n|^2 (\boldsymbol{u}_n - \boldsymbol{v}_n)\, f_n\, z\, d^3\boldsymbol{k} \quad (8b)$$

As the electron distribution function, $f_n(x,k,t)$, is not known (masked) in the HDM, the electron heat flux $\boldsymbol{Q}_n$ is usually approximated, with drastic assumptions. The majority of previous formulations of the HDM, made use of the Fourier law of heat conduction to approximate the electron heat flux [16]:

$$\boldsymbol{Q}_n = -k_n^{th} \nabla T_n, \quad (9a)$$

where k_n^{th} is the electron thermal conductivity. This law was originally developed for metals, where heat conduction is primarily carried out by electrons. Therefore, the electron thermal conductivity k_n^{th} is usually modeled by the Wiedeman-Franz law at the electronic temperature [1]:

$$k_n^{th} = \gamma_n\, (k_B/e)^2\, T_n\, \sigma_n, \quad (9b)$$

where σ_n is the electrical conductivity due to electrons and γ_n is the Lorenz coefficient for electrons. According to the original Wiedemann-Franz formulation [16], γ is given by [1]:

$$\gamma_n = 5/2 + r, \quad (9c)$$

where the parameter r depends on the dominant collision mechanism. The above treatment for modeling the carrier heat flux term (Q_n), using the Fourier relation, leads to many problems in the hydro-HD simulation of semiconductor devices [7].

In the our HDM, we rather utilize an advanced heat flux model, using the 3rd order moment of the BTE [16].

$$n\boldsymbol{F}.\langle ½\, u_n^2 + u_n \otimes u_n\rangle + + \nabla.(n\langle E_n\, u_n \otimes u_n\rangle) = -\frac{S_n}{\tau_{sn}}, \quad (10a)$$

where τ_{sn} is the energy flux relaxation time of electrons. The energy flux ($\boldsymbol{S}_n$) in the above conservation equation may be then divided into two parts, namely; the convection energy part (due to $\boldsymbol{J}_n$) and the heat conduction part $\boldsymbol{Q}_n$:

$$\boldsymbol{Q}_n = -3/2\ (k_B^2/e)\, \mu_{sn}\, \beta_n \nabla(n\, T_n^2) = =- k_n \nabla(n\, T_n^2), \quad (10b)$$

with

$$k_n = 3/2\ (k_B^2/e)\, \mu_{sn} \beta_n \quad (10c)$$

Also, μ_{sn} is the energy flux mobility of electrons (μ_{sn} = $e\tau_{sn}/m_n$) and the beta factor (β_n) is defined as follows:

$$\boldsymbol{\beta_n} = <E_n(\boldsymbol{u}_n - \boldsymbol{v}_n) \otimes \otimes (\boldsymbol{u}_n - \boldsymbol{v}_n)> / \omega_n <(\boldsymbol{u}_n - \boldsymbol{v}_n) \otimes (\boldsymbol{u}_n - \boldsymbol{v}_n)> \quad (10d)$$

As shown in Figs. 2a and 2b, both β_n and μ_{sn} can be determined by MC simulation in the bulk of a semiconductor [16]. When the carrier-concentration gradient is negligible, the above formula may be further reduced to a form similar to the conventional Fourier relation ($\boldsymbol{Q}_n$ = - $k_n^{th} \nabla\, T_n$). Therefore, the thermal conductivity due to electrons in a semiconductor is given by:

$$k_n^{th} = 3\ (k_B^2/e)\, n\, \mu_{sn}\, \beta_n)\, T_n = = 3\, \beta_n\, (k_B/e)^2\, (\mu_{sn}/\mu_n) \sigma_n\, T_n \quad (11a)$$

This relation is equivalent to the well-known Wiedeman-Franz relation (k_n^{th} = $\gamma_n (k_B/e)^2\, \sigma_n\, T_n$), with the following *modified' Lorenz parameter* (γ_n):

$$\gamma_n = 3\, \beta_n\, (\mu_{sn}/\mu_n) \quad (11b)$$

In the case of low electric field, where μ_{sn} = μ_n and β_n = 1, we can easily find that γ_n = 3, which

corresponds to the classic Wiedeman-Franz relation ($\gamma_n = 5/2+r$). This indicates that our model of heat flux is more versatile than the Fourier heat flux model. It also illustrates one of the error sources when adopting the Fourier law of heat conduction in semiconductor devices, to close the set of hydrodynamic equations.

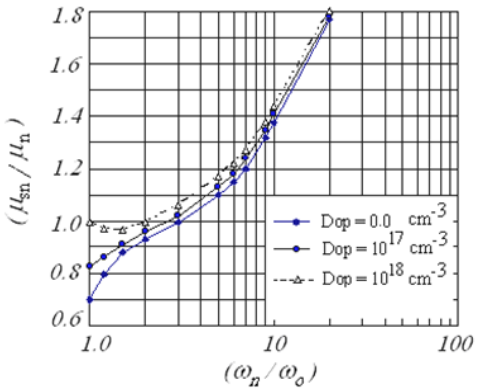

Fig. 2a. Relative energy flux mobility (μ_{sn}/μ_n) in Si at 300 K.

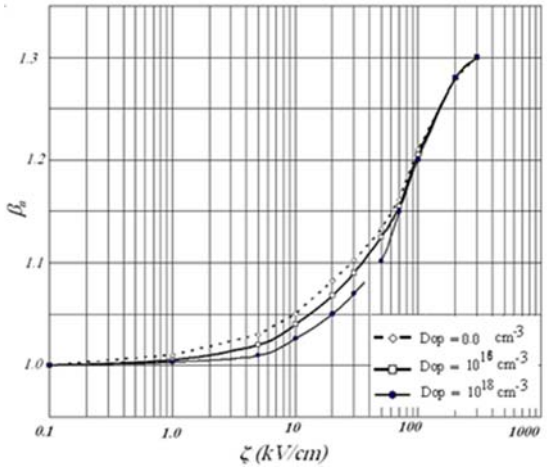

Fig. 2b. Heat flux beta factor in Si at 300K.

4. Final Set of HDE's

The final set of HDE's consists of the continuity equations of the carrier density (2a) and average carrier energy (2c), as well as the constitutive relations for the electron current density (7c) and energy flux (8a). Adding the quantum corrections [17], we can write:

$$\boldsymbol{J}_n = e\, n\, \mu_n \boldsymbol{\zeta} + \mu_n\, m_n\, \nabla.(g_n\, m_n^{-1}\, n\, k_B T_n) + \\ + n\, \mu_n\, m_n\, (v_n.\nabla)\, v_n + \boldsymbol{J}_{nq}, \tag{12a}$$

$$\boldsymbol{S}_n = \boldsymbol{Q}_n + n\, \boldsymbol{v}_n\, (\omega_n + k_B T_n), \tag{12b}$$

with

$$\omega_n = \tfrac{1}{2} m_n v_n^2 + 3/2\, k_B\, T_n + V_q \tag{12c}$$

The quantum correction potential (or Wigner potential [18]), V_q is given by:

$$V_q = \frac{\hbar^2}{8 m_n} \nabla^2 [ln\,(n)], \tag{13a}$$

and the quantum current correction is given by [17]:

$$J_{nq} = -e\, n\, \mu_n \left(\frac{\hbar^2}{6\, m_n}\right).\nabla\left(\frac{\nabla^2\sqrt{n}}{\sqrt{n}}\right) \tag{13b}$$

5. Energy-dependent Physical Parameters

The transport properties of hot carriers under high-field conditions are of great interest for high-power and high-speed semiconductor devices. Therefore, the accurate modeling of transport parameters at high fields is vital in any transport model. In the DDM, the transport parameters are usually expressed as functions of the local electric field. Nevertheless, some parameters such as the hot carrier mobility and impact ionization rate involve some non-local and energy exchange mechanisms that should better be expressed as functions of the average carrier energy, rather than the local electric field.

Fortunately, the solution of the HDM produces such information about the average carrier energy and permits to express these parameters in a physical manner, in semiconductor devices.

5.1. Energy-dependent Hot Carrier Drift Mobility

The electron drift mobility appears in the current density constitutive relation (4a). It can be expressed according to our advanced model [19]:

$$\mu_n^{-1} = \mu_{no}^{-1} \left[1 + \frac{\mu_{no}}{e\, n\, v_n^2}\left[\frac{n(\omega_n - \omega_o)}{\tau_{\omega n}} + \boldsymbol{A}.\nabla n + \right.\right. \\ \left.\left. + B.(\boldsymbol{v}.\nabla) v_n + \boldsymbol{C}.\nabla T_n + \boldsymbol{D}.\nabla m_n\right]\right], \tag{14a}$$

with

$$\boldsymbol{A} = m_n\, v_n^2 \boldsymbol{v}_n,\ B = -n\, m_n v_n, \\ \boldsymbol{C} = 3/2\, k_B\, n\, \boldsymbol{v}_n\, m_n\ \boldsymbol{D} = m_n^{-1}\, \tau_n n \boldsymbol{v}_n \tag{14b}$$

This model accounts for the non-local field effects on hot carrier transport, as well as other driving forces, due to gradient terms. In particular, the role of velocity gradients is depicted in Fig. 3, where the electron drift mobility of Si is plotted versus the average electron energy, at various values of the dimensionless parameter ($\tau_{wnn}\, \partial v_{ny}/\partial x$). It is clear from this figure that the electron gas viscosity plays a fundamental role in limiting the electron drift mobility near the surface of the semiconductor (e.g., the top surface of an n-channel planar MOSFET).

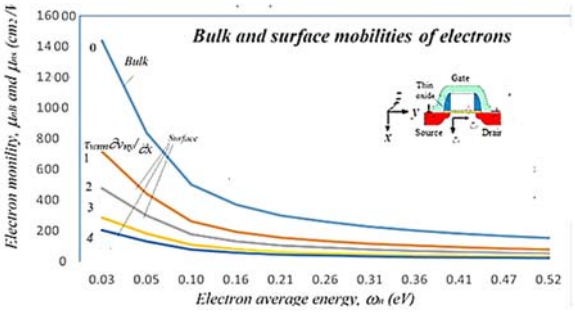

Fig. 3. Variation of the drift mobility of hot electrons, as a function of the electron average energy, and at various values of the velocity gradient ($\tau_{wn}\partial v_{ny}/\partial x$) near the surface of an n-channel MOSFET device. The low-field mobility u_{no} is assumed 1450 cm^2/V.s. After Taha and Saba [19].

5.2. Energy-dependent Impact Ionization Coefficient

The impact ionization is one of the generation mechanisms of charge carriers in semiconductors. The impact ionization phenomenon happens when colliding electrons have enough energy to ionize valence band electrons. The macroscopic impact ionization rate G_{ii} is usually expressed in terms of the impact ionization coefficients of electrons and holes, $\alpha_{n,p}$ [20].

$$G_{ii} = \alpha_n \, | J_n/e| + \alpha_p \, |J_p/e| \tag{15a}$$

The impact ionization rate of electrons, α, can be modelled as follows [21]:

$$\alpha_n(\omega_n) = \\ = \alpha_{no}.exp\left(-\frac{E_n^{I\square}}{(\omega_n-\omega_o)\left[1+\frac{(\omega_n-\omega_o)}{\eta_n E_p\square}\right]}\right), \tag{15b}$$

where $\alpha_{no} = (\omega_n\text{-}\omega_o)/(\lambda_n E_n^I)$, $E_n^I = \eta_n \; E_n^{th}$, $\eta_n = (v_n \tau_{wn}/\lambda_n)$ and E_n^{th} is the threshold ionization energy of electrons. Also, E_{ph} is the optical phonon energy and λ_n is the mean free path between electron collisions (of all scattering modes). Like $\tau_{\omega n}$ and m_n, λ_n can be expressed as a function of the mean carrier energy, by MC simulation in the bulk of semi-conductor.

At moderate average carrier energies, our impact ionization model reduces to:

$$\alpha_n(\omega_n) \approx \alpha_{no}.exp\left[-\frac{E_n^I}{(\omega_n-\omega_o)}\right] \tag{15c}$$

The above model is plotted in Fig. 3, and compared to other models. Unlike other models [21-25], the hard threshold energy (E_n^{th}) is replaced with a soft (energy-dependent) mean threshold energy (E_n^I) in our model. As shown in Fig. 4, this coincides with the conclusions of Bude and Hess about the impact ionization soft threshold energy [24].

At very low average electron energy, where $\omega_n - \omega_o = ½ m_n v_n^2$, there exists a certain probability of impact ionization. Therefore, the so-called low-voltage impact ionization, which was reported in the literature [25], is included implicitly in our model, via the convective energy.

At warm carrier regime the convective energy ($½ \; m_n v_n^2$) is usually in the order of acoustic phonon energy, E_{ac}, and may be much larger in certain device regions, due to velocity overshoots or ballistic transport. Therefore, it can increase the total electron energy above the threshold energy for impact ionization in nano MOSFET devices, even at low voltages.

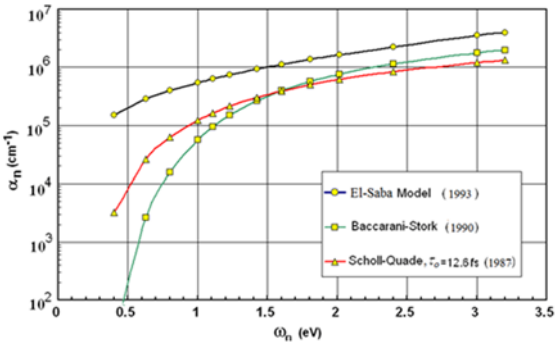

Fig. 4. Electron impact ionization rate in *Si* at 300K, as a function of average electron energy, according to Baccarani-Stork model *(λ_ω = 500Å, λ_o = 65Å)*, Scholl-Quade model *(τ_o = 14ps)* and our model. In all models, the threshold ionization energy $E_n^{th} = 1.2$ *eV*.

6. Results and Discussion

The Fig. 5 shows the hydrodynamic simulation results of an N-I-N structure, representing the source-channel-drain of an n-channel MOSFET. The results are compared with those obtained by other HDM's and MC device simulation. We note that the exaggerated velocity overshoot has been suppressed when using our proposed HDM. This is primarily due to the inclusion of the convective part of the average electron energy ($½ \; m_n \; vn^2$). This convection part is descending from the tensorial product term $(n \; \boldsymbol{v}_n \otimes \boldsymbol{v}_n)$, which is usually neglected in other formulations of the HDM. Such formulations are sometimes referred to as the energy-transport models (ETM). In fact the velocity gradient term $(v_n.\nabla) \; v_n$, which represents the acceleration / deceleration of electrons in the current density constitutive relation (4a), comes also from the divergence of this term $\nabla.(n \; \boldsymbol{v}_n \otimes \boldsymbol{v}_n)$. In addition, the off-diagonal elements ($v_{nj}\partial v_{ni}/\partial j$, with $i,j = x,y,z, \; i \neq j$) of the velocity gradient term, which appear in the electron mobility expression (14), are all about the electron gas viscosity. Therefore, keeping the convective transport components in our HDM is vital to capture many physical effects of the electron gas. Also, we note in Fig. 5 that the results obtained by our

HDM have more reasonable values of the electron temperature near high-field region, which are closer to MC simulation results. In fact, we can define an effective electron temperature, which combines the band structure and quantum corrections as follows:

$$T_{nm} = g_n T_n + 2/3 k_B V_{+q} \quad (16)$$

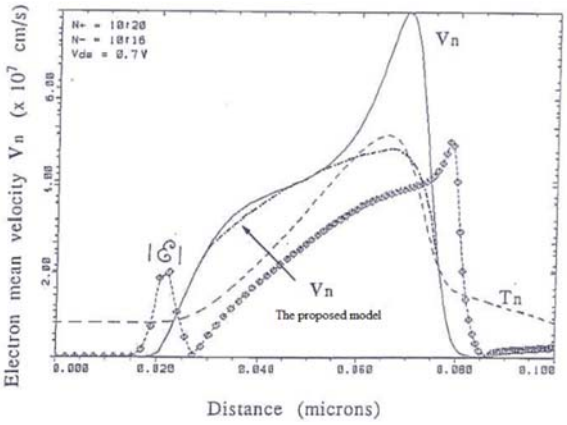

Fig. 5. Average electron velocity distributions across an N-N-I-N structure, according to our model and other models and Monte Carlo device simulation.

In another investigation of the proposed model, we simulated the bipolar transport of hot carriers across a two-dimensional reverse-biased P-I-N diode, The diode has a central (I) region of 64 um and uniform doping of 10^{14} cm^{-3}. Here, the conservation equations of carrier densities and average energies (for both electrons and holes) are solved with Poisson's equation. The Fig. 7 shows the electron and hole temperature distribution in 2D, under a reverse bias of 75 V. The surface effects are obvious near the upper surface of the diode Also, Fig. 6 show the energy flux distributions of electrons and holes of the same diode under a reverse bias of -500 V.

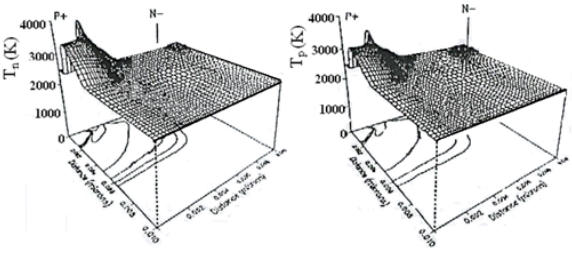

Fig. 6. Carrier temperature distributions across the P-I-N diode at reverse bias of 75 V.

7. Conclusions

In this paper, we proposed an advanced HDM for semi-conductors with arbitrary band structure and including electron gas viscosity and surface effects. There exists a few number of energy-dependent parameters, which can be determined by full-band MC simulation in the semiconductor of interest. Fortunately, almost all the model parameters are measurable physical quantities. In particular, the energy relaxation time captures the energy band structure and the dominant scattering mechanism, near the surface of semi-conductor [27]. The model has been appended with other transport models. The primary results are closer to the MC device simulation. For instance, the over-estimated electron velocity overshoot in nano-devices, has been relatively suppressed. The role of electron velocity gradients is emphasized and the underlined electron gas viscosity is therefore considered. The electron gas viscosity effects are particularly important to justify the mobility reduction near the surface of semi-conductor devices. Finally, the authors would like to attract the attention to the vital role of electron gas viscosity effects in semiconductor device modelling, which we think not reported yet in the [28]. Of course, more investigations about the proposed HDM and more comparisons with other approaches are required.

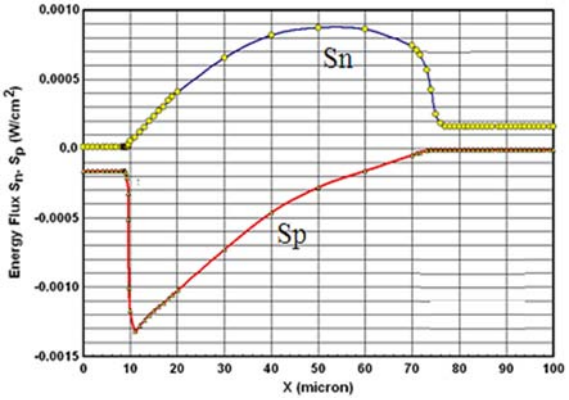

Fig. 7. Energy flux of electrons and holes along the P-I-N diode at 500 V reverse bias.

References

[1]. M. H. El-Saba, Transport of Information-Carriers in Semiconductors and Nanodevices, *IGI Global Publisher*, PA, USA, 2017.

[2]. B. Meinerzhagen, R. Thoma, H. J. Peifer, W. L. Engl, On the Consistency of the Hydro-dynamic and the Monte Carlo Models, http://www.researchgate.net/publication/37920832

[3]. M. Stettler, M. Alam, M. Lundstrom, A Critical examination of the assumptions underlying macroscopic transport equations for silicon devices, *IEEE Trans. Electron. Dev.*, Vol. 40, Issue 4, 1993, pp. 733-740.

[4]. C. Jungemann, T. Grass, B. Neinhilus, B. Meeinerzhagen, Failure of moments-based transport models in nanoscale devices near equilibrium, *IEEE Trans. Electron. Dev.*, Vol. 52, Issue 11, November 2005, pp. 2404-2408.

[5]. G. Wolodkin, J. Frey, Overshoot effects in the relaxation time approximation, in *Proceedings of the Eight International Conference on the Numerical*

Analysis of Semiconductor Devices and Integrated Circuits NASCODE VIII, Vienna, 1992, pp. 107-108.

[6]. M. H. El-Saba, Accurate estimation of electron velocity overshoots in sub-0.1 micron silicon structures and MOSFET devices, in *Proceedings of the 15th Radio Science Conference (NRSC'98)*, 1998, pp. D2/1-D2/5.

[7]. D. Chen, E. C. Kan, U. Ravaioli, W.-C. Shu, R. W. Dutton, An improved energy transport model including non-parabolicity and non-Maxwellian distribution effects, *IEEE Trans. Electron. Dev. Lett*., Vol. 13, Issue 1, 1992, pp. 26-28.

[8]. M. H. El-Saba, Accurate Non-local modeling of hot-carriers drift mobility in semiconductor devices, in *Proceedings of the 8th Int. Conference on Microelectronics*, Cairo, 1996.

[9]. M. H. El-Saba, Problems related to the semiconductors hydrodynamic model: modeling the carrier-heat flux term, in *Proceedings of the 8th Int. Conference on Microelectronics*, Cairo, 1996, pp. 162-166.

[10]. V. Romano, Non-parabolic band hydrodynamic model of silicon semiconductors and simulation of electron devices, *Mathematical Methods in the Applied Sciences*, Vol. 24, Issue 7, 2001, pp. 439-471.

[11]. C. Jacoboni, P. Lugli, The Monte Carlo Method for Semi-conductor Device Simulation, *Springer Science*, 2012.

[12]. A. J. Sabbah, D. M. Riffe, Femto-second pump-probe reflectivity study of silicon carrier dynamics, *Phys. Rev. B*, Vol. 66, 2002, pp. 165217-165228.

[13]. B. Gonzalez, V. Palankovsk, H. Kosina, A. Hernandez, S. Selberherr, An analytical energy relaxation time model for device simulation, *Solid-State Electron*, Vol. 43, 1999, pp. 1791-1795.

[14]. E. Sermuknis, J. Liberis, A. Matulionis, Microwave noise technique for measurement of hot-electron energy relaxation time and hot-phonon lifetime, *Lithuanian Journal of Physics*, Vol. 47, Issue 4, 2007, pp. 491-498.

[15]. M. Mohyee-Edin, K. Sehrawy, M. S. Taha, M. H. EL-Saba, Electro-kinetic pressure correction parameter of hydrodynamic model calculation, using Monte Carlo simulation, in *Proceedings of the International Conference on Microelectronic Devices and Technologies (MicDAT'24)*, Ibiza, Spain, 25-27 Sept. 2024 (submitted).

[16]. K. W. Böer, U. W. Pohl, Semiconductor Physics. *Springer*, 2018.

[17]. A. Jüngel, D. Matthes, A derivation of the isothermal quantum hydrodynamic equations using entropy minimization, Z. angew. Math. Mech., Vol. 85, 2005, pp. 806-814.

[18]. D. K. Ferry, S. Ramey, L. Shifren, E. Alkis, The effective potential in device modeling: the good, the bad and the ugly, *Journal of Comp. Electron*., Vol. 1, Issue 1, 2002, pp. 59-65.

[19]. M. S. Taha, M. H. EL-Saba, A unified mobility model, including band structure and semiconductor surface effects, in *Proceedings of the International Conference on Microelectronic Devices and Technologies (MicDAT'24)*, Ibiza, Spain, 25-27 Sept. 2024 (submitted).

[20]. M. H . El-Saba, Yet another hydrodynamic model for silicon devices with correlated parameters, scientific and academic publishers, *Microelectronic Devices and Solid-State Electronics*, Vol. 1, Issue 5, 2012, pp. 118-147.

[21]. M. H. El-Saba, Accurate modeling of energy-dependent impact ionization rate for hydrodynamic simulators of semiconductor devices, in *Proceedings of the IEEE Radio Science Conference (NRSC'99)*, 23-25 Feb. 1999, pp. D2/1-D2/5.

[22]. E. Schöll, W. Quade, Effect of impact ionisation on hot-carrier energy and momentum relaxation in semiconductors, *J. Phys. C: Solid State Phys.*, Vol. 20, 1987, pp. L861-L867.

[23]. E. F. Crabbé, H. Stork, G. Baccarani, M. V. Fischetti, S. E. Laux, The impact of non-equilibrium transport on breakdown and transit time in bipolar transistors, in *Proceedings of the International Electron Devices Meeting*, 1990.

[24]. P. Su, K-I. Goto, T. Sugii, C. Hu, A thermal activation view of low voltage impact ionization in MOSFETs, *IEEE Electron. Dev. Let*., Vol. 23, Issue 9, 2002, pp. 550-552.

[25]. J. Bude, K. Hess, Threshold of impact ionization in semiconductors, *J. Appl. Phys*., Vol. 72, Issue 8, 1992, 3554.

[26]. N. Nida, U. Grossner, High temperature impact-ionization model for 4H-SiC, *IEEE Trans. E. Devices*, Vol. 66, Issue 4, 2019, pp. 1899-1904.

[27]. J. Billiald, D. Backes, J. König, I. Farrer, D. Ritchie, V. Narayan, Determining energy relaxation length scales in two-dimensional electron gases, *Applied Physics Letters*, Vol. 107, 2015, 022104.

[28]. P. S. Alekseev, A. P. Dmitriev, Viscosity of two-dimensional electrons, *arXiv Preprint*, 2021, arXiv:2007-02291v4.